Biochimica et Biophysica Acta 1848 (2015) 127–133

Contents lists available at ScienceDirect

Biochimica et Biophysica Acta

journal homepage: www.elsevier.com/locate/bbamem

Structural characterization of novel cationic diC16-amidine bilayers: Evidence for partial interdigitation

Julio H.K. Rozenfeld [a,*], Evandro L. Duarte [a], Jean-Marie Ruysschaert [b], Caroline Lonez [b], M. Teresa Lamy [a]

[a] Instituto de Física, Universidade de São Paulo, São Paulo, Brazil
[b] Service de Structure et Fonction des Membranes Biologiques, Université Libre de Bruxelles, Bruxelles, Belgium

ARTICLE INFO

Article history:
Received 25 July 2014
Received in revised form 25 September 2014
Accepted 2 October 2014
Available online 12 October 2014

Keywords:
Partial interdigitation
Electron spin resonance
Differential scanning calorimetry
diC16-amidine
Membrane fusion
Fluorescence resonance energy transfer

ABSTRACT

In this work, the bilayer structure of novel cationic lipid diC16-amidine was compared to the one of zwitterionic dipalmitoyl phosphatidylcholine (DPPC), which shares the same hydrophobic domain.
Differential scanning calorimetry shows that DPPC and diC16-amidine bilayers have similar phase transition temperatures, but diC16-amidine membranes display a less cooperative phase transition and an absence of pretransition.
Both bilayers were analyzed from surface to core, using 5-, 7-, 10-, 12-, 14-, and 16-PCSL spin labels. As expected, electron spin resonance (ESR) spectra show that the gel phase of DPPC presents a flexibility gradient toward the core. In contrast, this gradient exists in the gel phase of diC16-amidine bilayers but only down to the 12th lipid tail carbon. The 14th and 16th carbons of the cationic lipid are in a very rigid environment, similar to the one observed at the bilayer surface. These data suggest that diC16-amidine molecules are organized in a partially interdigitated gel phase. ESR spectroscopy also shows that the lamellar fluid phase of diC16-amidine is more rigid than the one of DPPC.
Fluorescence resonance energy transfer assays reveal that diC16-amidine displays a more efficient fusogenic activity in the gel phase than in the fluid one, suggesting that the partial interdigitation of the gel phase is important for the fusion process to occur. Since the gel–fluid transition temperature is 42 °C, diC16-amidine is fusogenic at the physiological temperature and is therefore a promising lipid for delivery applications without the need of helper lipids.

1. Introduction

Liposomes have become of huge importance in medicine and healthcare [1]. Over a dozen of liposome formulations have been approved for human use [2], offering suitable treatment for a series of diseases such as fungal infections [3,4], leishmaniasis [5], macular degeneration [6] and cancer [7–9]. They have also been employed in vaccine [10–12] and imaging [13,14] applications. This has prompted the development and characterization of new synthetic lipids, like cationic lipids [15,16].

A family of cationic lipids containing the amidine group was synthesized some 25 years ago [17] to deliver nucleic acids intracellularly [18,19]. Studies carried out with 14-carbon lipid tailed diC14-amidine demonstrated its capacity to enhance lipid mixing [20], and also to activate the innate immune system [21,22].

The high fusogenic efficiency of diC14-amidine bilayers was correlated with the presence of an interdigitated gel phase [20], in which lipid molecules were packed side by side and flipped horizontally from one to the other [23,24].

It was previously shown that diC16-amidine, a 16-carbon lipid tail derivative of diC14-amidine, fuses more efficiently than diC14-amidine with cell membranes at 37 °C [25]. Hence, characterizing the structural and biological properties of diC16-amidine could expand the applications of the amidine lipid family.

In this work, the structure of cationic diC16-amidine bilayers was characterized and compared to the structure of bilayers formed by dipalmitoyl phosphatidylcholine (DPPC), a zwitterionic lipid that has the same hydrophobic domain. The fusogenic activity of diC16-amidine was also assessed as a function of temperature. Differential scanning calorimetry (DSC), electron spin resonance (ESR) spectroscopy and fluorescence resonance energy transfer (FRET) were employed in this study.

2. Materials and methods

2.1. Reagents

Texas Red®-DHPE (Texas Red® 1,2-dihexadecanoyl-*sn*-glycero-3-phospho-ethanolamine, triethylammonium salt) and NBD-PE (*N*-(7-nitrobenz-2-oxa-1,3-diazol-4-yl)-1,2- dihexadecanoyl-*sn*-glycero-3-phospho-ethanolamine, triethylammonium salt) are Invitrogen

* Corresponding author. Tel.: +55 11 3091 6953.
E-mail address: julioroz@if.usp.br (J.H.K. Rozenfeld).

http://dx.doi.org/10.1016/j.bbamem.2014.10.013
0005-2736/

(Molecular Probes) products. Hepes (4-(2-hydroxyethyl) piperazine-1-ethanesulfonic acid)) was purchased from Sigma Chemical Co. (St. Louis, MO, USA). DPPC (dipalmitoyl phosphatidylcholine), asolectin (L-α-phosphatidylcholine (Soy-20%)) and spin labels 1-palmitoyl-2-(*n*-doxylsearoyl)-*sn*-glycero-3-phosphocholine (*n*-PCSL, $n = 5, 7, 10, 12, 14$, or 16) were supplied by Avanti Polar Lipids (Birmingham, AL, USA). diC16-amidine (3-tetradecylamino-*N*-*tert*-butyl-*N*′-hexadecyl-propionamidine) was synthesized as described [17] and stored as a powder at −20 °C. The chemical structures of DPPC, diC16-amidine and 10-PCSL are shown in Fig. 1. Ultrapure water of Milli-Q-Plus quality was used throughout.

2.2. Liposome preparation

A lipid film was formed from a chloroform solution, dried under a stream of N_2, and left under reduced pressure for a minimum of 2 h, to remove all traces of organic solvent. Dispersions were prepared by addition of Hepes buffer (10 mM, pH 7.4) followed by vortexing for about 5 min at 50 °C. For ESR experiments, 0.8 mol% 5-PCSL, 0.6 mol% 7-PCSL, 0.5 mol% 10-PCSL, 0.4 mol% 12-PCSL, 0.3 mol% 14-PCSL, or 0.3 mol% 16-PCSL were added to the lipid chloroform solutions when preparing the lipid films. No spin–spin interaction was observed at such small label concentrations. For fluorescence measurements, NBD-PE and Texas Red-DHPE® (at 0.8 mol% each) were dissolved with diC16-amidine in chloroform before lipid film formation. Final diC16-amidine concentrations were 0.85 μM, 2 mM and 10 mM for FRET, DSC, and ESR experiments, respectively. All samples were used right after preparation.

2.3. Differential scanning calorimetry (DSC)

DSC scans were performed in a Microcal VP-DSC Microcalorimeter (Microcal Inc., Northampton, MA, USA) equipped with 0.5 mL twin total-fill cells. Heating rates were 20 °C/h. Scans were performed at least in duplicate. The enthalpy of transition ΔH was obtained by integrating the area under the thermograms.

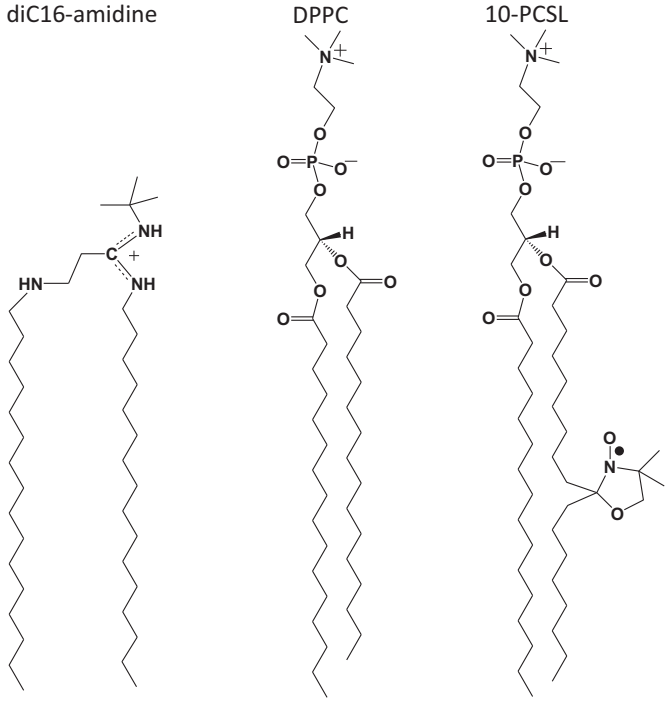

Fig. 1. Chemical structures of diC16-amidine, DPPC and 10-PCSL.

2.4. Electron spin resonance (ESR) spectroscopy

ESR measurements at X-band were performed with a Bruker EMX spectrometer. Field-modulation amplitude of 1G and microwave power of 5 mW were used. The temperature was controlled to about 0.2 °C with a Bruker BVT-2000 variable temperature device, and monitored with a Fluke 51 K/J thermometer with a probe placed just above the cavity. A high sensitivity ER4119HS cavity was used. All ESR data shown are means of the results of at least two experiments, and the uncertainties are the standard deviations. When not shown, the uncertainty was found to be smaller than the symbol in the graph.

The effective order parameter, S_{eff}, was calculated from the expression [26]

$$S_{eff} = \frac{A_{//} - A_{\perp}}{A_{ZZ} - (1/2)\left(A_{xx} + A_{yy}\right)} \frac{a_o'}{a_o}$$

where $a_o' = (1/3)(A_{xx} + A_{yy} + A_{zz})$, $a_o = (1/3)(A_{//} + 2A_{\perp})$, $A_{//}$ $(= A_{max})$ is the maximum hyperfine splitting directly measured in the spectrum (see Fig. 6), $A_{\perp} = A_{min} + 1.4\left[1 - \frac{A_{//} - A_{min}}{A_{zz} - (1/2)(A_{xx} + A_{yy})}\right]$, A_{min} is the measured minimum hyperfine splitting (see Fig. 6) and A_{xx}, A_{yy} and A_{zz} are the principal values of the hyperfine tensor for doxylpropane [27].

Rotational correlation times for isotropic motion, according to the motional narrowing theory, can be calculated from the peak-to-peak width of the ESR Lorentzian lines [28,29]:

$$\Delta H_L(m) = A + Bm + Cm^2$$

where m is the m-th component of the nitrogen nuclear spin, A is the Lorentzian linewidth of the central line, $\Delta H_L(0)$, and B and C are

$$B = \frac{1}{2}\Delta H_L(0)\left(\frac{\Delta H_L(+1)}{\Delta H_L(0)} - \frac{\Delta H_L(-1)}{\Delta H_L(0)}\right)$$

$$C = \frac{1}{2}\Delta H_L(0)\left(\frac{\Delta H_L(+1)}{\Delta H_L(0)} + \frac{\Delta H_L(-1)}{\Delta H_L(0)} - 2\right).$$

The correlation time for doxyl labels can be calculated using both B and C parameters: $\tau_B = -1.22\ B$ or $\tau_C = 1.19\ C$, ($\tau_B = \tau_C$ for isotropic movement). Lorentzian linewidths are calculated using a computer program, which performs nonlinear least-square fitting of the experimental ESR spectrum using a model of a Lorentzian–Gaussian function for corrections of non-resolved hyperfine splitting [30,31]. This methodology can only be applied to ESR spectra yielded by probes in the motional narrowing regime [30]. In the present work, it could only be applied to 16-PCSL. The average rotational correlation time $\overline{\tau}$ corresponds to the arithmetic mean of τ_B and τ_C.

2.5. Lipid mixing assay

Lipid mixing between cationic diC16-amidine liposomes and asolectin liposomes was monitored using Fluorescence Resonance Energy Transfer (FRET) assay. Cationic liposomes were labeled with NBD-PE and Texas Red®-DHPE as described above. Asolectin liposomes were added to labeled diC16-amidine liposomes at a mass ratio of 10:1 and loaded in a quartz thermostatized fluorescence cell. The samples were gently stirred throughout the experiment. The fluorescence was monitored using an SLM-8000 spectrofluorometer with excitation and emission slits of 4 nm. Generally, samples were excited at 470 nm and emission spectra were recorded between 500 nm and 625 nm. Control emission spectra were performed in parallel before and after lipid mixing. For each temperature, the percentage of fusion was calculated as the ratio between the NBD donor emission fluorescence (532–

538 nm) intensity of the sample at that temperature and the average donor emission fluorescence intensity after adding 1% Triton X-100 over all the temperature range. Addition of the Triton detergent destabilizes the liposomes and mimics a 100% fusion.

3. Results and discussion

3.1. Thermotropic behavior of DPPC and diC16-amidine

diC16-amidine and DPPC share the same hydrophobic domain made of 16-carbon alkyl chains but have different hydrophilic moieties (a small cationic headgroup for diC16-amidine and a larger zwitterionic headgroup for DPPC) (Fig. 1). These lipids have similar transition temperatures of 42 °C for diC16-amidine and 41 °C for DPPC (Fig. 2). However, their transition profiles are very different: while DPPC has a very sharp gel–fluid transition, diC16-amidine has a very broad one, indicating a much smaller transition cooperativity for the cationic lipid bilayers (Fig. 2).

The decrease in transition cooperativity for diC16-amidine membranes could be attributed to electrostatic repulsion between cationic headgroups that destabilizes the gel phase at low ionic strength. This is consistent with the smaller transition enthalpy of diC16-amidine ($\Delta H = 6.7$ kcal/mol) as compared with DPPC ($\Delta H = 8.8$ kcal/mol). A broad phase transition for anionic DPPG bilayers was previously attributed to repulsion between negatively charged headgroups [32].

It is also interesting to note that diC16-amidine does not present the pretransition observed for DPPC at 34 °C (Fig. 2), or observed for other cationic and anionic lipids at different temperatures below the phase transition [33,34]. The disappearance of the pretransition has been reported for several interdigitated phases [35–38], including diC14-amidine membranes [20].

3.2. Structural comparison of diC16-amidine and DPPC gel phase membranes

Phospholipids spin-labeled at different positions along the hydrocarbon chain were used to probe the organization of diC16-amidine and DPPC membranes. ESR spectra of 5-, 7-, 10-, 12-, 14-, and 16-PCSL inserted into the gel phase (T = 15 °C) of these membranes are shown in Fig. 3.

For DPPC, spectra profiles change significantly from bilayer surface to core: spectra of 5- and 7-PCSL, located near the lipid–water interface, are significantly more anisotropic than those of 14- and 16-PCSL, which

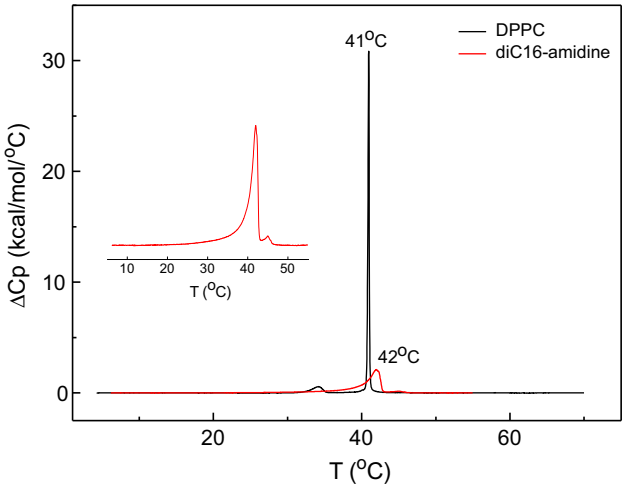

Fig. 2. Thermograms of diC16-amidine and DPPC. Lipid concentration was 2 mM. Phase transition temperatures are indicated. Scan rate was 20 °C/h. Inset shows a zoom of diC16-amidine thermogram.

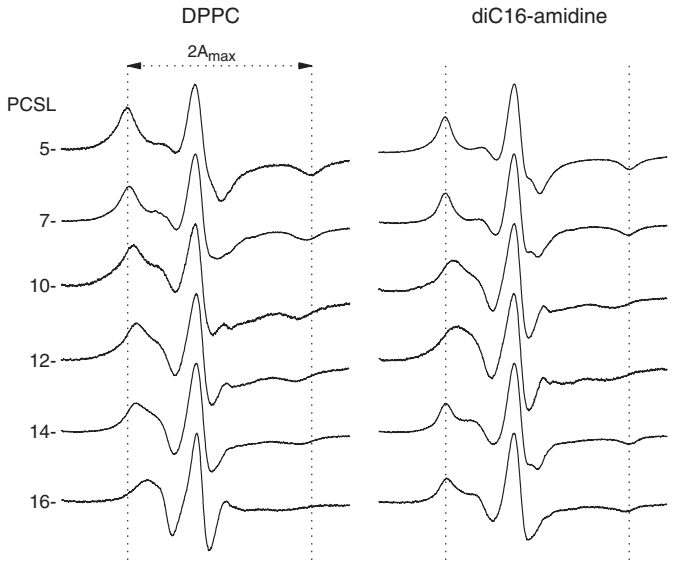

Fig. 3. ESR spectra of 5-, 7-, 10-, 12-, 14-, and 16-PCSL incorporated in DPPC and diC16-amidine, at 15 °C. Dotted lines indicate the positions of the maximum hyperfine splitting (A_{max}) of the 5-PCSL spectra. Total spectra width is 100 G.

are deeply inserted into the bilayer hydrophobic core (Fig. 3). This confirms the existence of a bilayer flexibility gradient [27,39], in which carbons located deeper in the bilayer present less organization and more freedom of motion even in the bilayer gel phase.

For diC16-amidine, spectra anisotropy also decreases from 5- to 12-PCSL (Fig. 3). However, spectra of 14- and 16-PCSL and of 5- and 7-PCSL are very similar. The anisotropic features of these spectra suggest that the probes buried deeper in the diC16-amidine bilayer are in a more rigid (less fluid) microenvironment than those located in the middle of the alkyl chains, such as 10- and 12-PCSL (Fig. 3).

In order to quantitatively evaluate these differences, it is possible to use the maximum hyperfine splitting, A_{max}. This parameter is directly measured on the spectra (Fig. 3) and is sensitive to the label microenvironment viscosity or packing [40]. Since both chain order and mobility are evaluated, A_{max} measures the fluidity of the membrane. Hence, in general, A_{max} values decrease as temperature increases (Fig. 4).

DPPC displays a typical bilayer pattern as A_{max} decreases when the paramagnetic moiety is located deeper into the bilayer (Fig. 4A). This means that even in the gel phase the alkyl chains are not totally extended in the all-trans conformation, and this is in agreement with the flexibility gradient mentioned above.

A decrease in A_{max} values is also observed for diC16-amidine bilayers, but only between 5- and 12-PCSL probes (Fig. 4B). The A_{max} values for 14- and 16-PCSL are higher and similar to the ones recorded for 5- and 7-PCSL (Fig. 4B). This indicates that membrane fluidity increases between the 5th and the 12th carbon, but sharply decreases for the 14th and 16th carbons, as concluded from the spectra profiles (Fig. 3).

ESR probes located near the bilayer core have been successfully employed to diagnose the existence of interdigitated organization: in this case, they are more motionally restricted and/or ordered than non-interdigitated bilayers and have parameters similar to the probes near the bilayer surface [26,41]. It is precisely the pattern observed with diC16-amidine.

For symmetric lipids, interdigitation is mainly caused by interfacial perturbations induced by substances like alcohol [42,43], acetonitrile [44], glycerol and polymyxin B [26], and by charge effects [45–48].

The lipid structure also plays an important role in the formation of interdigitated phases in symmetric lipids: the synthetic 1,3-DPPC isomer displays an interdigitated gel phase due to increased intramolecular chain separation when compared to DPPC [49,50].

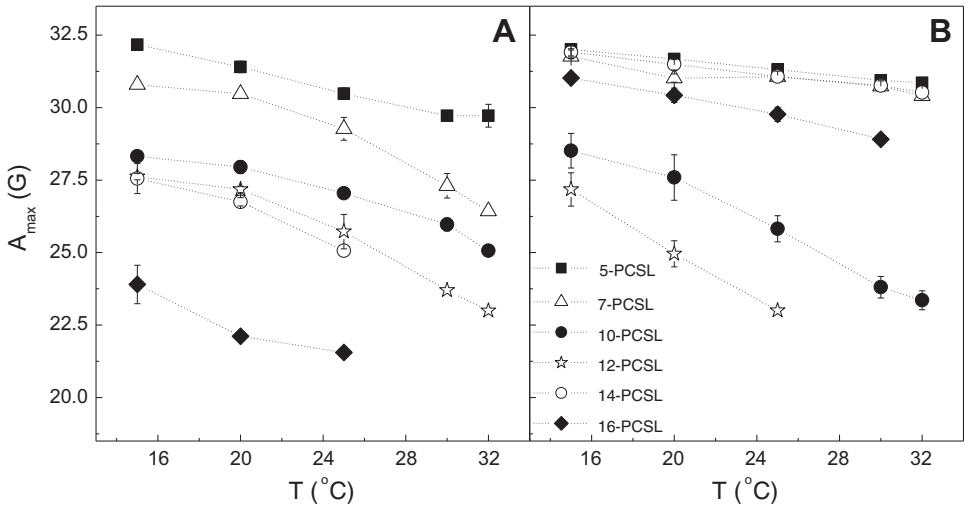

Fig. 4. Maximum hyperfine splitting (A_{max}) measured from the ESR spectra of 5- (■), 7- (△), 10- (●), 12- (☆), 14- (○), and 16-PCSL (◆) incorporated in the gel phase of (A) DPPC and (B) diC16-amidine.

Similarly, the large intramolecular chain separation due to an extra CH_2 group is responsible for the adjacent interdigitation of diC14-amidine gel phase, in which lipid molecules are packed side by side and flipped horizontally from one to the other [23,24].

This adjacent interdigitated phase was characterized using a series of ESR probes [20]. All the five probes used (5-, 7-, 10-, 12-, and 16-PCSL) presented a very narrow range of high A_{max} values. In the case of diC16-amidine, the membrane is rigid near the surface and the core, but displays flexibility similar to the DPPC around the 10th and 12th carbon (Figs. 3 and 4). This shows that the gel phase structures of diC16-amidine and diC14-amidine are different.

Since the extra CH_2 separating the amine and amidine groups is also present in diC16-amidine molecules (Fig. 1), interdigitation is not completely abolished even in the presence of longer lipid tails: instead of the complete interdigitation observed for diC14-amidine bilayers, diC16-amidine bilayers might present a partial interdigitation (Fig. 5). This partial interdigitation could result from the energetic balance between enhanced van der Waals interactions of longer lipid tails and electrostatic repulsion of cationic headgroups. The presence of a partial interdigitation may explain the absence of pretransition in diC16-amidine bilayers observed in Fig. 2, as previously mentioned.

3.3. Structural comparison of diC16-amidine and DPPC fluid phase membranes

Fig. 6 shows the ESR spectra of spin labels inserted into the fluid phase (T = 50 °C) of diC16-amidine or DPPC membranes. In both membranes, the spectra become less anisotropic, i.e., more fluid, toward the bilayer core, as expected for lamellar (non-interdigitated) fluid phases. Hence, in contrast to the gel phase, the fluid phase of both DPPC and diC16-amidine bilayers display a flexibility gradient toward the membrane core.

For the fluid phase, distinct parameters were used to analyze the spectra of the different spin labels. The effective order parameter (S_{eff}) is an appropriate parameter to evaluate lipid chain order with 5- and 7-PCSL probes (Fig. 7). Due to the position of their nitroxide group closer to the bilayer surface, these labels present rapid anisotropic molecular motion, and both the maximum and minimum hyperfine splitting (A_{max} and A_{min}, respectively) can be directly measured [27], as shown in Fig. 6. As described in Materials and methods, calculated S_{eff} values depend on both A_{max} and A_{min} values [51]. S_{eff} includes contributions

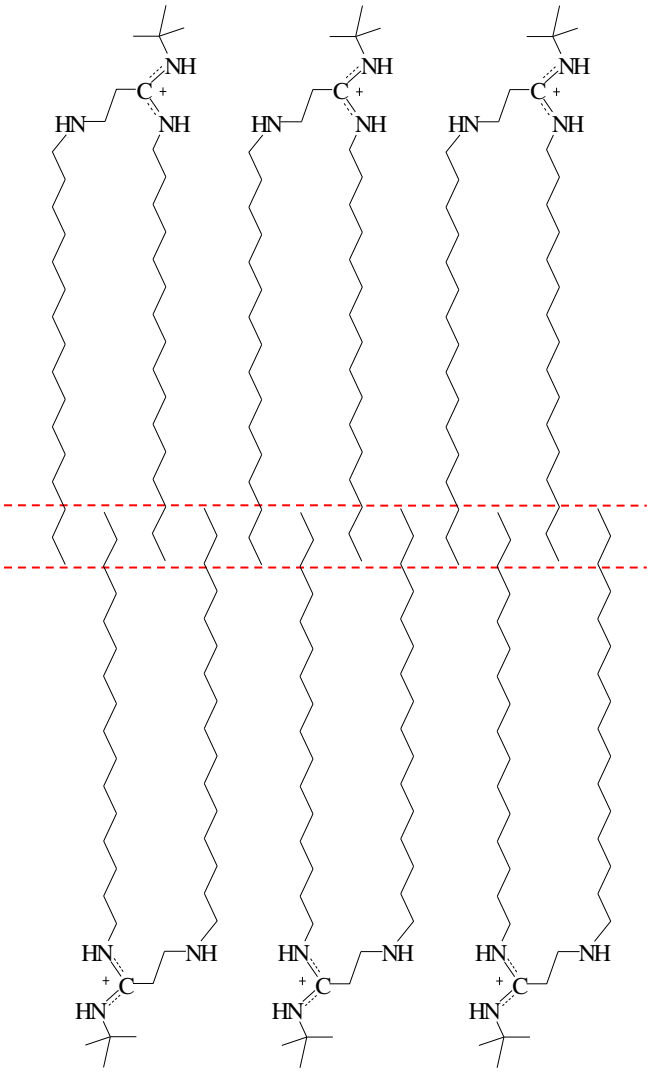

Fig. 5. Scheme of partial interdigitation in diC16-amidine bilayers. Dashed lines highlight the interdigitation region.

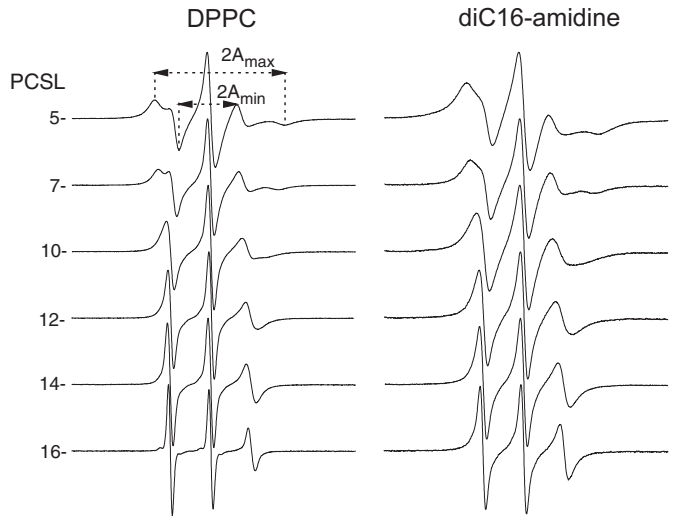

Fig. 6. ESR spectra of 5-, 7-, 10-, 12-, 14-, and 16-PCSL incorporated in DPPC and diC16-amidine, at 50 °C. Maximum and minimum hyperfine splittings (A_{max} and A_{min}) are indicated. Total spectra width is 100 G.

from chain order and rate of motion, but the main contribution is the amplitude of segmental motion of the acyl chains [51].

S_{eff} values are higher for diC16-amidine than for DPPC membranes (Fig. 7), showing that the membrane surface of the cationic lipid is more packed. A similar effect was observed when comparing diC14-amidine and DMPC [20].

Spin labels located deeper in the bilayer, such as 10-, 12-, 14-, and 16-PCSL, sense a less ordered microenvironment and yield more isotropic signals from which A_{max} and A_{min} cannot be accurately measured (see Fig. 6). However, rotational correlation times can be accurately obtained from the fitting of the spectra using a Lorentzian–Gaussian function, as described in Materials and methods (Section 2.4). Good fitting can only be obtained in the motional narrowing regime [30], which is the case for the 16-PCSL probe.

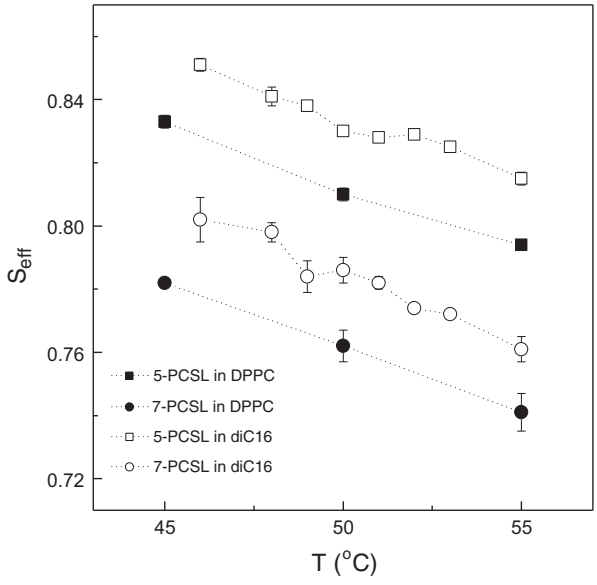

Fig. 7. Effective order parameter (S_{eff}) measured on ESR spectra of 5-PCSL (squares) and 7-PCSL (circles) inserted in the fluid phase of DPPC (full symbols) or diC16-amidine (open symbols) liposomes.

Table 1
Rotational correlation times and standard errors (s.e.) for 16-PCSL in the fluid phase of DPPC and diC16-amidine bilayers calculated from spectra shown in Fig. 6.

	$\tau_B \pm$ s.e. (ns)	$\tau_C \pm$ s.e. (ns)	$\overline{\tau}$ (ns)
DPPC	0.56 ± 0.01	0.48 ± 0.01	0.52
diC16-amidine	0.57 ± 0.01	0.62 ± 0.01	0.59

Due to the difficulty in establishing a nitroxide preferential rotational axis [52], the values of two rotational correlation times, τ_B and τ_C, were calculated from spectra using the B and C parameters described in Section 2.4, and were corrected for the contribution of non-resolved hyperfine splittings [30]. The slightly different values of τ_B and τ_C presented in Table 1 indicate a rotation anisotropy of the 16-PCSL probe that is expected in lipid bilayers [29]. Hence, an average rotational correlation time, $\overline{\tau}$ (Table 1), can be used to evaluate the bilayer packing, since rotational correlation time values increase with packing.

The value of $\overline{\tau}$ is about 13% higher in diC16-amidine than in DPPC bilayers (Table 1), showing that the bilayer core of diC16-amidine bilayers is more packed than that in DPPC bilayers. Hence, S_{eff} and $\overline{\tau}$ data show that the fluid phase of diC16-amidine is more rigid than that of DPPC (Fig. 7 and Table 1).

It is also interesting to mention that the S_{eff} and τ_B and τ_C values for diC16-amidine at 50 °C (Fig. 7 and Table 1) are higher than those obtained for diC14-amidine [53]. This implies that the fluid phase of diC16-amidine is also more packed than the one of diC14-amidine. This is an expected consequence of enhanced hydrophobic interactions in a lipid with longer alkyl chains.

3.4. Effect of temperature on the fusion of diC16-amidine and asolectin liposomes

The fusion of diC16-amidine and asolectin liposomes was monitored at different temperatures using fluorescence resonance energy transfer (FRET). Lipid mixing efficiency is expressed as the percentage of fusion after 30 min of incubation (Fig. 8).

Lipid mixing is more efficient at temperatures below 40 °C, i.e., at the gel phase (Fig. 8). This suggests that the interdigitated organization is very important for the fusion process, as previously described for ethanol-induced interdigitated phospholipid vesicles [43,54,55].

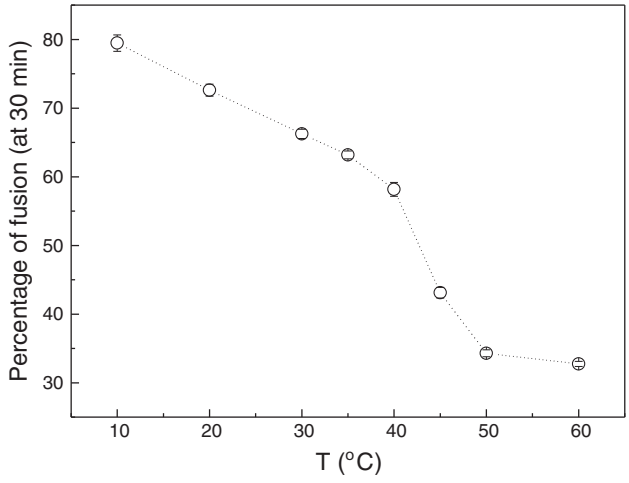

Fig. 8. Effect of temperature on lipid mixing efficiency after 30 min of incubation between diC16-amidine and asolectin liposomes expressed as the percentage of fluorescence intensity at 532–538 nm as compared to the fluorescence intensity observed after adding 1% Triton X-110 to the sample (mimicking 100% fusion efficiency). Results are representative of three independent assays and errors represent standard deviation.

A similar phenomenon of enhanced fusion with interdigitated gel phase has been described for diC14-amidine [20]. However, diC16-amidine has a broader temperature range of improved efficiency, and can be employed at the physiological temperature of 37 °C (Fig. 8). In fact, at this temperature, diC16-amidine is in the partially interdigitated gel phase while diC14-amidine already adopts a lamellar fluid organization, and that might explain the higher fusogenic activity of the former at this condition [25]. It is also worth noticing that fusion induced by viruses, peptides and hexagonal phase-promoting phospholipids (such as DOPE) is usually enhanced at higher, and not lower, temperatures [56–60].

It was recently shown that optimizing membrane fusion conditions might have a dramatic impact in siRNA delivery [61]. In this context, the high fusogenic efficiency of diC16-amidine at physiological condition without the need of helper lipids suggests a very promising application for this novel cationic lipid.

4. Conclusions

DPPC and diC16-amidine bilayers have similar phase transition temperatures of 41 °C and 42 °C, respectively. However, diC16-amidine membranes display a less cooperative phase transition, and no pretransition is observed for these cationic membranes.

Spin labels show that the gel phase of DPPC bilayers presents a flexibility gradient from surface to core, as expected. In contrast, diC16-amidine bilayers present a flexibility gradient from the 5th to the 12th lipid tail carbons, whereas the carbons located at the 14th and 16th positions are in a very rigid environment. Such rigidity at the membrane core suggests the formation of a partially interdigitated gel phase. This partial interdigitation could be the consequence of a large intramolecular separation of lipid tails, and might explain the absence of pretransition in diC16-amidine bilayers.

ESR spectroscopy also shows that lamellar fluid phases are present in both DPPC and diC16-amidine membranes. However, the bilayers are more rigid for the fluid phase of diC16-amidine.

FRET assays show that diC16-amidine bilayers display an efficient fusogenic activity at the gel phase, implying that the interdigitated organization of this phase, even if partial, is important for the fusion process. The fusogenic activity of diC16-amidine is very efficient at the physiological temperature of 37 °C suggesting its use as a promising lipid for delivery applications under physiological conditions without the need of helper lipids.

Acknowledgements

This work was supported by USP, FAPESP, CNPq and FNRS. J.H.K.R. is a FAPESP fellow (2011/13079-9). C.L. is a Marie Curie Fellow.

References

[1] Y. Zhang, H.F. Chan, K.W. Leong, Advanced materials and processing for drug delivery: the past and the future, Adv. Drug Deliv. Rev. 65 (2013) 104–120.
[2] T.M. Allen, P.R. Cullis, Liposomal drug delivery systems: from concept to clinical applications, Adv. Drug Deliv. Rev. 65 (2013) 36–48.
[3] I.M. Hann, H.G. Prentice, Lipid-based amphotericin B: a review of the last 10 years of use, Int. J. Antimicrob. Agents 17 (2001) 161–169.
[4] R. Bowden, P. Chandrasekar, M.H. White, X. Li, L. Pietrelli, M. Gurwith, J.A. van Burik, M. Laverdiere, S. Safrin, J.R. Wingard, A double-blind, randomized, controlled trial of amphotericin B colloidal dispersion versus amphotericin B for treatment of invasive aspergillosis in immunocompromised patients, Clin. Infect. Dis. 35 (2002) 359–366.
[5] R.N. Davidson, L. Di Martino, L. Gradoni, R. Giacchino, R. Russo, G.B. Gaeta, R. Pempinello, S. Scott, F. Raimondi, A. Cascio, T. Prestileo, L. Caldeira, R.J. Wilkinson, A.D.M. Bryceson, Liposomal amphotericin B (AmBisome) in Mediterranean visceral leishmaniasis: a multi-centre trial, Q. J. Med. 87 (1994) 75–81.
[6] N.M. Bressler, V.I.P.T.S. Group, Verteporfin therapy of subfoveal choroidal neovascularization in age-related macular degeneration: two-year results of a randomized clinical trial including lesions with occult with no classic choroidal neovascularization — verteporfin in photodynamic therapy report 2, Am J. Ophthalmol. 131 (2001) 541–560.
[7] Y. Barenholz, Doxil® — the first FDA-approved nano-drug: lessons learned, J. Control. Release 160 (2012) 117–134.
[8] C.E. Petre, D.P. Dittmer, Liposomal daunorubicin as treatment for Kaposi's sarcoma, Int. J. Nanomedicine 2 (2007) 277–288.
[9] M.A. Rodriguez, R. Pytlik, T. Kozak, M. Chhanabhai, R. Gascoyne, B. Lu, S.R. Deitcher, J.N. Winter, Vincristine sulfate liposomes injection (Marqibo) in heavily pretreated patients with refractory aggressive non-Hodgkin lymphoma: report of the pivotal phase 2 study, Cancer 115 (2009) 3475–3482.
[10] D.S. Watson, A.N. Endsley, L. Huang, Design consideration for liposomal vaccines: influence of formulation parameters on antibody and cell-mediated immune responses to liposome associated antigens, Vaccine 30 (2012) 2256–2272.
[11] J.H.K. Rozenfeld, S.R. Silva, P.A. Ranéia, E. Faquim-Mauro, A.M. Carmona-Ribeiro, Stable assemblies of cationic bilayer fragments and CpG oligonucleotide with enhanced immunoadjuvant activity in vivo, J. Control. Release 160 (2012) 367–373.
[12] A. Wilmar, C. Lonez, M. Vermeersch, M. Andrianne, D. Pérez-Morga, J.M. Ruysschaert, M. Vandenbranden, O. Leo, S.T. Temmerman, The cationic lipid, diC14-amidine, extends the adjuvant properties of aluminum salts through a TLR-4- and caspase-1-independent mechanism, Vaccine 30 (2012) 414–424.
[13] B.A. Goins, W.T. Phillips, The use of scintigraphic imaging as a tool in the development of liposome formulations, Prog. Lipid Res. 40 (2001) 95–123.
[14] M. Dunne, J. Zheng, J. Rosenblat, D.A. Jaffray, C. Allen, APN/CD13-targeting as a strategy to alter the tumor accumulation of liposomes, J. Control. Release 154 (2011) 298–305.
[15] S.L. Hart, Lipid carriers for gene therapy, Curr. Drug Deliv. 2 (2005) 423–428.
[16] C.T. Ilarduya, Y. Sun, N. Düzgünes, Gene delivery by lipoplexes and poliplexes, Eur. J. Pharm. Sci. 40 (2010) 159–170.
[17] F. Defrise-Quertain, P. Duquenoy, R. Brasseur, P. Brak, B. Caillaux, R. Fuks, J.M. Ruysschaert, Vesicle formation by double long-chain amidines, J. Chem. Soc. Chem. Commun. 14 (1986) 1060–1062.
[18] J.M. Ruysschaert, A. El Ouahabi, V. Willeaume, G. Huez, R. Fuks, M. Vandenbranden, P. Di Stefano, A novel cationic amphiphile for transfection of mammalian cells, Biochem. Biophys. Res. Commun. 203 (1994) 1622–1628.
[19] A. El Ouahabi, V. Pector, R. Fuks, M. Vandenbranden, J.M. Ruysschaert, Double long-chain amidine liposome-mediated self replicating RNA transfection, FEBS Lett. 380 (1996) 108–112.
[20] T.R. Oliveira, E.L. Duarte, M.T. Lamy, M. Vandenbranden, J.M. Ruysschaert, C. Lonez, Temperature-dependence of cationic lipid bilayer intermixing: possible role of interdigitation, Langmuir 28 (2012) 4640–4647.
[21] T. Tanaka, A. Legat, E. Adam, J. Steuve, J.S. Gatot, M. Vandenbranden, L. Ulianov, C. Lonez, J.M. Ruysschaert, E. Muraille, M. Tuynder, M. Goldman, A. Jacquet, DiC14-amidine cationic liposomes stimulate myeloid dendritic cells through Toll-like receptor 4, Eur. J. Immunol. 38 (2008) 1351–1357.
[22] C. Lonez, M. Vandenbranden, J.M. Ruysschaert, Cationic lipids activate intracellular signal pathways, Adv. Drug Deliv. Rev. 64 (2012) 1749–1758.
[23] G. Pabst, C. Lonez, M. Vandenbranden, J. Jestin, A. Radulescu, J.M. Ruysschaert, T. Gutberlet, Stalk-free membrane fusion of cationic lipids via an interdigitated phase, Soft Matter 8 (2012) 7243–7249.
[24] J.H.K. Rozenfeld, E.L. Duarte, T.R. Oliveira, C. Lonez, J.M. Ruysschaert, M.T. Lamy, Oligonucleotide adsorption affects phase transition but not interdigitation of diC14-amidine bilayers, Langmuir 29 (2013) 11102–11108.
[25] C. Lonez, M.F. Lensink, E. Kleiren, J.M. Vanderwinden, J.M. Ruysschaert, M. Vandenbranden, Fusogenic activity of cationic lipids and lipid shape distribution, Cell. Mol. Life Sci. 67 (2010) 483–494.
[26] J.M. Boggs, G. Rangaraj, Phase transitions and fatty acid spin label behavior in interdigitated lipid phases induced by glycerol and polymyxin, Biochim. Biophys. Acta 816 (1985) 221–233.
[27] W.L. Hubbel, H.M. McConnell, Molecular motion in spin-labeled phospholipids and membranes, J. Am. Chem. Soc. 93 (1971) 314–326.
[28] J.H. Freed, G.K. Fraenkel, Theory of linewidths in electron spin resonance spectra, J. Chem. Phys. 39 (1963) 326–348.
[29] S. Schreier, C.F. Polnaszek, I.C. Smith, Spin labels in membranes. Problems in practice, Biochim. Biophys. Acta 515 (1978) 395–436.
[30] B. Bales, Inhomogeneously Broadened Spin-label Spectra, in: L.J. Berliner, J. Reuben (Eds.), Spin labeling, Theory and applications, vol. 8, Plenum Press, New York, 1989, pp. 77–130.
[31] H.J. Halpern, M. Peric, C. Yu, B.L. Bales, Rapid quantitation of parameters from inhomogeneously broadened EPR spectra, J. Magn. Res. Ser. A 103 (1993) 13–22.
[32] K.A. Riske, R.P. Barroso, C.C. Vequi-Suplicy, R. Germano, V.B. Henriques, M.T. Lamy, Lipid bilayer pre-transition as the beginning of the melting process, Biochim. Biophys. Acta 1788 (2009) 954–963.
[33] J. Cocquyt, U. Olsson, G. Olofsson, P. Van der Meeren, Thermal transitions of DODAB vesicular dispersions, Colloid Polym. Sci. 283 (2005) 1376–1381.
[34] R.P. Barroso, K.A. Riske, V.B. Henriques, M.T. Lamy, Ionization and structural changes of the DMPG vesicle along its anomalous gel – fluid phase transition: a study with different lipid concentrations, Langmuir 26 (2010) 13805–13814.
[35] L.F. Braganza, D.L. Worcester, Hydrostatic pressure induces hydrocarbon chain interdigitation in single-component phospholipid bilayers, Biochemistry 25 (1986) 2591–2596.
[36] D.J. Hirsh, N. Lazaro, L.R. Wright, J.M. Boggs, T.J. McIntosh, J. Schaefer, J. Blazyk, A new monofluorinated phosphatidylcholine forms interdigitated bilayers, Biophys. J. 75 (1998) 1858–1868.
[37] C. Matsingou, C. Demetzos, Calorimetric study on the induction of interdigitated phase in hydrated DPPC bilayers by bioactive labdanes and correlation to their liposome stability: the role of chemical structure, Chem. Phys. Lipids 145 (2007) 45–62.
[38] J.A. Veiro, P. Nambi, L.L. Herold, E.S. Rowe, Effect of n-alcohols and glycerol on the pretransition of dipalmitoylphosphatidylcholine, Biochim. Biophys. Acta 900 (1987) 230–238.

[39] J.H. Davis, Deuterium magnetic resonance study of the gel and liquid crystalline phases of dipalmitoyl phosphatidylcholine, Biophys. J. 27 (1979) 339–358.
[40] J.H. Freed, in: L.J. Berliner (Ed.), Spin labeling: theory and applications, Academic Press, New York, 1976, pp. 53–132.
[41] J.M. Boggs, G. Rangaraj, A. Watts, Behavior of spin labels in a variety of interdigitated lipid bilayers, Biochim. Biophys. Acta 981 (1989) 243–253.
[42] S.A. Simon, T.J. McIntosh, Interdigitated hydrocarbon chain packing causes the biphasic transition behavior in lipid/alcohol suspensions, Biochim. Biophys. Acta 773 (1984) 169–172.
[43] H. Komatsu, S. Okada, Ethanol-induced aggregation and fusion of small phosphatidylcholine liposome: participation of interdigitated membrane formation in their processes, Biochim. Biophys. Acta 1235 (1995) 270–280.
[44] F.G. Wu, N.N. Wang, L.F. Tao, Z.W. Yu, Acetonitrile induces nonsynchronous interdigitation and dehydration of dipalmitoylphosphatidylcholine bilayers, J. Phys. Chem. B 114 (2010) 12685–12691.
[45] R.N. Lewis, I. Winter, M. Kriechbaum, K. Lohner, R.N. McElhaney, Studies of the structure and organization of cationic lipid bilayer membranes: calorimetric, spectroscopic, and X-ray diffraction studies of linear saturated P-O-ethyl phosphatidylcholines, Biophys. J. 80 (2001) 1329–1342.
[46] I. Winter, G. Pabst, M. Rappolt, K. Lohner, Refined structure of 1,2-diacyl-P-O-ethylphosphatidylcholine bilayer membranes, Chem. Phys. Lipids 112 (2001) 137–150.
[47] W. Pohle, C. Selle, D.R. Gauger, R. Zantl, F. Artzner, J.O. Radler, FTIR spectroscopic characterization of a cationic lipid–DNA complex and its components, Phys. Chem. Chem. Phys. 2 (2000) 4642–4650.
[48] S.J. Ryhanen, J.M. Alakoskela, P.K. Kinnunen, Increasing surface charge density induces interdigitation in vesicles of cationic amphiphile and phosphatidylcholine, Langmuir 21 (2005) 5707–5715.
[49] E.N. Serrallach, R. Dijkman, G.H. de Haas, G.G. Shipley, Structure and thermotropic properties of 1,3-dipalmitoyl-glycero-2-phosphocholine, J. Mol. Biol. 170 (1983) 155–174.
[50] A. Zumbuehl, B. Dobner, G. Brezesinski, Phase behavior of selected artificial lipids, Curr. Opin. Colloid Interface Sci. 19 (2014) 17–24.
[51] H. Schindler, J. Seelig, EPR spectra of spin labels in lipid bilayers, J. Chem. Phys. 59 (1973) 1841–1850.
[52] D. Marsh, Experimental Methods in Spin-label Spectral Analysis, in: L.J. Berliner, J. Ruben (Eds.), Spin labeling, Theory and applications, vol. 8, Plenum Press, New York, 1989, pp. 255–303.
[53] C.R. Benatti, J.M. Ruysschaert, M.T. Lamy, Structural characterization of diC14-amidine, a pH-sensitive cationic lipid used for transfection, Chem. Phys. Lipids 131 (2004) 197–204.
[54] P.L. Ahl, L. Chen, W.R. Perkins, S.R. Minchey, L.T. Boni, T.F. Taraschi, A.S. Janoff, Interdigitation–fusion: a new method for producing lipid vesicles of high internal volume, Biochim. Biophys. Acta 1195 (1994) 237–244.
[55] P.L. Ahl, W.R. Perkins, Interdigitation–fusion liposomes, Methods Enzymol. 367 (2003) 80–98.
[56] S. Frey, M. Marsh, S. Gunther, A. Pelchen-Mathews, P. Stephens, S. Ortlepp, T. Stegmann, Temperature dependence of cell–cell fusion induced by the envelope glycoprotein of human immunodeficiency virus type 1, J. Virol. 69 (1995) 1462–1472.
[57] A.M. Haywood, B.P. Boyer, Time and temperature dependence of influenza virus membrane fusion at neutral pH, J. Gen. Virol. 67 (1986) 2813–2817.
[58] S. Mondal, M. Sarkar, Non-steroidal anti-inflammatory drug induced membrane fusion: concentration and temperature effects, J. Phys. Chem. B 113 (2009) 16323–16331.
[59] S.A. Wharton, J.J. Skehel, D.C. Wiley, Temperature dependence of fusion by Sendai virus, Virology 271 (2000) 71–78.
[60] H. Ellens, D.P. Siegel, D. Alford, P.L. Yeagle, L. Boni, L.J. Lis, P.J. Quinn, J. Benrtz, Membrane fusion and inverted phases, Biochemistry 28 (1989) 3692–3703.
[61] J.J. Lu, R. Langer, J. Chen, A novel mechanism is involved in cationic lipid-mediated functional siRNA delivery, Mol. Pharm. 6 (2009) 763–771.